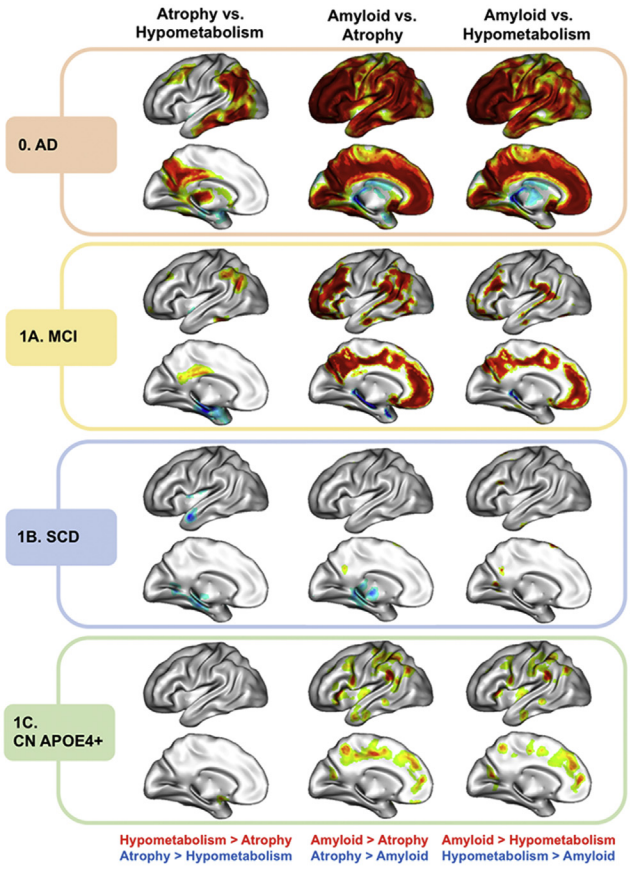

Figure 1. Voxel-wise intra-modality comparisons between regional degrees of atrophy, hypermetabolism and amyloid deposition in diagnostic groups with 1A. Mild Cognitive Impairment (MCI), 1B. Subjective Memory Decline (SCD), 1C. CN APOE4 carriers as well as 0. AD patients (for visual comparison). Contrast maps were displayed on the left hemisphere thresholded at t -values of $p < 0.001$ uncorrected, k = 20.

fluorodeoxyglucose PET and 18F-florbetapir PET data were collected from Aβ-negative/neurodegeneration-negative CN controls (n=41, 66±8 years), CN APOE4 carriers (n=17, 64±9 years), and patients with SCD (n=16, 69±7 years), MCI (n=30, 73±7 years) and AD (n=22, 69±9 years). For each imaging modality, standardized age-adjusted maps were computed using the controls as reference group. Relative degrees of biomarker expression were assessed in each diagnostic group via voxel-wise inter-modality comparisons of standardized maps. In addition, discriminatory power of AAL ROIs preferentially sensitive to Aβ deposition, hypometabolism, or atrophy (as derived in AD patients) was examine. **Results:** In the MCIs voxel-wise analyses detected AD-typical patterns in the relative degree of biomarker expressions (Figure 1a). In SCD only predominant medial-temporal atrophy was recovered (Figure 1b), while CN APOE4 carriers showed greater degree of Aβ deposition (Figure 1c). Confirming these findings, MCI patients were discriminated from controls by Aβ deposition-, hypometabolism-, and atrophy-predominant ROIs. Only the atrophy-predominant ROI distinguished SCD patients, and only the Aβ deposition-predominant ROI discriminated CN APOE4 carriers. **Conclusions:** MCI patients exhibit regional variation in the relative degree of Aβ deposition, hypometabolism, and atrophy typically seen in AD, although less extended and pronounced. SCD appears to reflect pathological mechanisms linked to atrophy in the absence of Aβ deposition. CN APOE4 carriers predominately harbor Aβ pathology without AD-typical patterns of atrophy or hypometabolism. Our findings suggest that Aβ and non-Aβ pathways could emerge first in different at-risk groups and converge in prodromal AD.

IC-01-04 DIAGNOSTIC IMPACT OF [^{18}F]FLUTEMETAMOL AMYLOID IMAGING IN YOUNG-ONSET DEMENTIA

Marissa D. Zwan[1,2], Femke Bouwman[1,2], Elles Konijnenburg[1,2], Wiesje M. van der Flier[1,2], Adriaan A. Lammertsma[1,2], Bart N.M. van Berckel[1,2], Philip Scheltens[1,2], *[1]VU University Medical Center, Amsterdam, Netherlands; [2]Neuroscience Campus Amsterdam, Amsterdam, Netherlands. Contact e-mail: m.zwan@vumc.nl*

Background: In young onset dementia, approximately one out of three patients has an atypical clinical presentation, which substantially complicates correct nosological diagnosis. *In vivo* detection of amyloid pathology can be useful in the diagnostic process. The present study aimed to examine the diagnostic impact of the amyloid-PET imaging agent [^{18}F]flutemetamol in assessing patients with young onset dementia. **Methods:** The present study included 200 patients visiting our tertiary memory clinic and diagnosed with young onset dementia (age <70 years). Patients were enrolled when physician's diagnostic confidence was <90% after a full routine diagnostic work-up for dementia. All patients underwent a [^{18}F]flutemetamol PET scan which was visually assessed as amyloid positive or negative. Scans were performed 90-110 minutes after injection of 185 MBq [^{18}F]flutemetamol. Before and after disclosing PET results to the physician, clinical diagnosis and confidence in this diagnosis were determined. In addition, the impact on healthcare management plan, including medication and care, and request for additional investigations was assessed. **Results:** [^{18}F]Flutemetamol scans were positive in 107 out of 137 (78%) patients with a pre-PET AD diagnosis and in 20 out of 63 (32%) patients diagnosed with a non-AD dementia prior to PET. Overall, confidence in diagnosis increased in 87% of the patients, on average from 69±12% to 89±15% after disclosing PET results (p<0.001). In 68 (34%) patients, [^{18}F]flutemetamol PET results led to a change in patient healthcare management (i.e. medication changed in 61 patients and care plan altered in 22 patients). A positive PET scan resulted in change of management plans (either medication, care, or both) nine times more often than a negative PET scan (n=61 vs. n=7; p<0.001). For 43 (22%) patients, additional ancillary investigations were planned after PET results were disclosed, predominantly when PET results were negative (n=33; p<0.001). In patients with a pre-PET AD diagnosis and a positive PET scan, additional ancillary investigations were less often requested compared to patients with a negative PET scan (p<0.001). **Conclusions:** [^{18}F]Flutemetamol PET increased physician's overall confidence in clinical diagnosis. In

addition, it altered diagnostic work-up and healthcare management plan of young onset dementia patients visiting a tertiary memory clinic.

IC-01-05 *IN VIVO* BRAAK STAGING USING 18F-AV1451 TAU PET IMAGING

Michael Schöll[1,2], Daniel Schonhaut[3], Sam Lockhart[1], Jacob W. Vogel[1], Suzanne Baker[4], Henry Schwimmer[1], Rik Ossenkoppele[3,5], Gil D. Rabinovici[3], William J. Jagust[1], *[1]University of California Berkeley, Berkeley, CA, USA; [2]University of Gothenburg, Gothenburg, Sweden; [3]University of California San Francisco, San Francisco, CA, USA; [4]Lawrence Berkeley National Laboratory, Berkeley, CA, USA; [5]VU University Amsterdam, Amsterdam, Netherlands. Contact e-mail: Michael.Scholl@neuro.gu.se*

Background: Alzheimer's disease (AD) related tau pathology has previously been classified into six consecutive Braak stages describing the gradual regional deposition of hyperphosphorylated tau protein over the course of the disease. Positron emission tomography (PET) using the ligand 18F-AV1451 (previously T807) now renders possible the *in vivo* assessment and staging of tau pathology and its relationship with cerebral glucose metabolism as measured with 18F-FDG. **Methods:** Nineteen elderly and two young normal controls (NCs), as well as eight AD patients (Table 1), underwent 18F-AV1451 PET scanning (80-100 min tissue ratio, cerebellar gray matter reference). Structural magnetic resonance (MR) images were co-registered to the respective PET images and segmented into regions of interest (ROIs) corresponding anatomically to the transentorhinal (I/II), limbic (III/IV), and isocortical (V/VI) Braak stages using FreeSurfer v5.1 (Figure 1). High AV1451 binding was identified by calculating a ratio of voxels > 2 SD above NC mean over total voxel count within each ROI. In addition, seventeen NCs and five AD patients also received 18F-FDG PET scans (30-60 min tissue ratio, pontine reference). **Results:** We found clear separation of NCs from AD patients throughout all Braak stages (Figure 2). Linear regression identified higher AV1451 uptake in early stage Braak ROIs as being highly predictive of higher uptake in later stage Braak ROIs, independent of ApoE status or age (Figure 3). Furthermore, linear regression of mean 18F-AV1451 uptake in Braak ROIs on 18F-FDG uptake in a predefined set of ROIs covering regions typically susceptible for AD-related hypometabolism yielded significant negative relationships in Braak ROIs I/II and III/IV. **Conclusions:** Our findings demonstrate the potential of tau PET imaging with 18F-AV1451 as a marker of AD-related tau pathology in the context of traditional cross-sectional Braak staging. Higher binding in early stage Braak ROIs suggests higher uptake in later stage Braak ROIs. In addition, higher 18F-AV1451 uptake in earlier stage Braak ROIs (I/II and III/IV) appeared to predict lower glucose metabolism in regions typically exhibiting AD-related hypometabolism in our population of NCs and AD patients, highlighting a spatially disentangled relationship between early Braak stage tau pathology and decreased cerebral glucose metabolism.

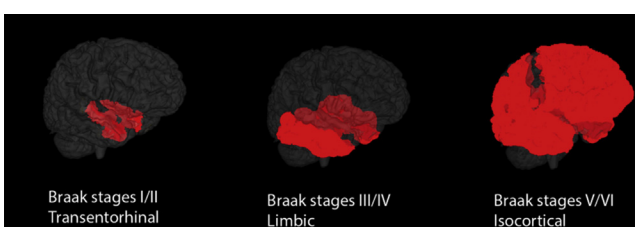

Figure 1. Combined FreeSurfer ROIs

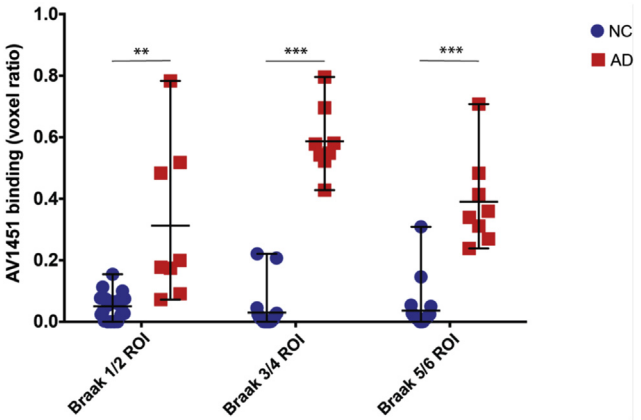

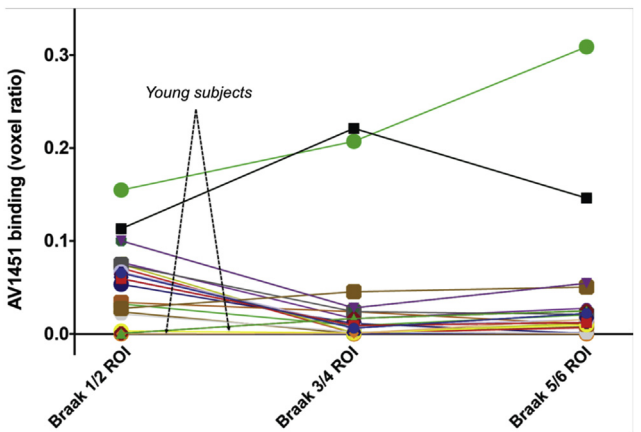

Table 1
Demographics

	NC (n=21)	AD (n=8)
Age	73 ± 10.6	66.3 ±8.2
Education	13.2 ±6.2	16.1 ±2.5
MMSE	28.9 ±1.2	22.3 ±4.9
ApoE ε4 (0/1/2/na)	11/5/0/5	2/1/2/3
Gender	13F/8M	6F/2M